

Field-induced spin-flop transitions in single-crystalline CaCo_2As_2

B. Cheng, B. F. Hu, R. H. Yuan, T. Dong, A. F. Fang, Z. G. Chen, G. Xu, Y. G. Shi, P. Zheng, J. L. Luo, and N. L. Wang
Institute of Physics, Chinese Academy of Sciences, Beijing 100080, People's Republic of China
 (Received 12 November 2011; revised manuscript received 2 April 2012; published 25 April 2012)

CaCo_2As_2 , a ThCr_2Si_2 -structure compound, undergoes an antiferromagnetic transition at $T_N = 76$ K with the magnetic moments being aligned parallel to the c axis. Electronic transport measurement reveals that the coupling between conducting carriers and magnetic order in CaCo_2As_2 is much weaker compared to the parent compounds of iron pnictide. Applying magnetic field along the c axis induces two successive spin-flop transitions in its magnetic state. The magnetization saturation behaviors with $\mathbf{H} \parallel c$ and $\mathbf{H} \parallel ab$ at 10 K indicate that the antiferromagnetic coupling along the c direction is very weak. The interlayer antiferromagnetic coupling constant J_c is estimated to be about 2 meV.

DOI: [10.1103/PhysRevB.85.144426](https://doi.org/10.1103/PhysRevB.85.144426)

PACS number(s): 75.30.Cr, 75.50.Ee, 74.70.Xa

I. INTRODUCTION

Magnetic responses of magnetic materials to external fields have been one of the most active fields in condensed-matter physics due to their enormous value for fundamental researches and practical applications. Competition between exchange energy, magnetocrystalline anisotropy energy, and Zeeman energy could introduce many fascinating magnetic phenomena in magnetic materials.^{1,2} Especially, in an antiferromagnet with low anisotropy, a magnetic field applied parallel to the easy axis could induce a transition to a phase in which the magnetic moments lie in a direction perpendicular to the external magnetic field. This is the so-called spin-flop transition. Spin-flop phenomena have been observed in many magnetic materials,³⁻⁶ including many low-dimensional antiferromagnets.⁷⁻¹⁰

Recently, the discovery of high- T_c iron pnictide superconductors opens a playground for the community to explore the magnetism and its interplay with superconductivity.¹¹ Most parent compounds of FeAs-based superconductors exhibit a long-range antiferromagnetic (AFM) order at low temperature. Similar to the cuprates, hole or electron doping will suppress AFM and introduce superconductivity.^{12,13} In the 1111 family, T_c reaches up to 55 K,¹⁴ which is much higher than the value expected from the traditional electron-phonon coupling theory. It is widely believed that the superconductivity in iron pnictides has an unconventional origin.

Moderate hole or electron doping will destroy the long-range antiferromagnetic order in iron pnictide parents. However, a complete substitution of Fe by Co in ReFeAsO ($\text{Re} = \text{La-Gd}$) will introduce complex magnetic phenomena. LaCoAsO shows ferromagnetic (FM) order below 55 K with a saturation moment of 0.3–0.4 μ_B per Co atom.¹⁵ In ReCoAsO ($\text{Re} = \text{Ce-Gd}$), the existence of 4*f* electrons in rare-earth elements leads to extra complexity in magnetism.^{15,16} Recent neutron-diffraction experiments reveal NdCoAsO undergoes three magnetic transitions: (a) a ferromagnetic transition at 69 K from Co moments, (b) a transition from FM to AFM at 14 K, and (c) an antiferromagnetic order of Nd 4*f* moments below 1.4 K.^{17,18} Neutron experiments indicate that all ordered moments lie in the ab plane. The moments on Co atoms in each CoAs layer are ferromagnetically ordered, and these layers are aligned antiferromagnetically along the c direction. The two Nd sites in each NdO layer are aligned antiferromagnetically

and alternate in direction between layers. The interplay between 3*d* and 4*f* electrons may play an important role in these successive magnetic transitions.

However, BaCo_2As_2 , which belongs to the 122 family, exhibits paramagnetic behavior above 1.8 K.¹⁹ The enhancement of susceptibilities relative to the weak correlated electron systems indicates that BaCo_2As_2 is close to a magnetic quantum critical point. In this article, we report our exploration of single-crystalline CaCo_2As_2 . Different from BaCo_2As_2 , we found that CaCo_2As_2 undergoes an antiferromagnetic transition at 76 K with magnetic moments being aligned parallel to the c axis. Interestingly, applying a magnetic field parallel to the easy axis induces two successive spin-flop transitions in its magnetic state. Our studies indicate that the magnetic coupling between the ab plane is very weak, so that the magnetic ground state of CaCo_2As_2 can be disturbed easily by a moderate external magnetic field.

II. EXPERIMENTAL DETAIL

CaCo_2As_2 single crystals were grown by a self-flux method similar to the procedures described in many references.^{19,20} The typical crystal size was $\sim 5 \times 5 \times 0.1$ mm³. Resistivity and specific-heat measurements were performed on a Quantum Design physical property measurement system (PPMS). dc magnetization was measured as functions of temperature and magnetic field using a Quantum Design instrument superconducting quantum interference device (SQUID-VSM) and PPMS.

III. RESULTS AND DISCUSSIONS

Figure 1 shows susceptibilities in 5 kOe along the c axis and ab plane. The susceptibility for $\mathbf{H} \parallel c$ exhibits a sharp peak at $T_N = 76$ K and drops rapidly with decreasing temperature, indicative of an antiferromagnetic transition with the magnetic moments being aligned parallel to the c axis.⁴ Susceptibility for $\mathbf{H} \parallel ab$ shows a peak around 76 K, too, but it does not decrease rapidly as $\mathbf{H} \parallel c$ and shows nearly no temperature dependence below T_N . Above 150 K, the susceptibilities follow the Curie-Weiss law very well. The inset of Fig. 1 shows Curie-Weiss fits to the high-temperature parts of the susceptibilities. These fits give a Weiss temperature of $\theta_{ab} = 98$ K for $\mathbf{H} \parallel ab$ and $\theta_c = 65$ K for $\mathbf{H} \parallel c$. The effective moment of Co is calculated

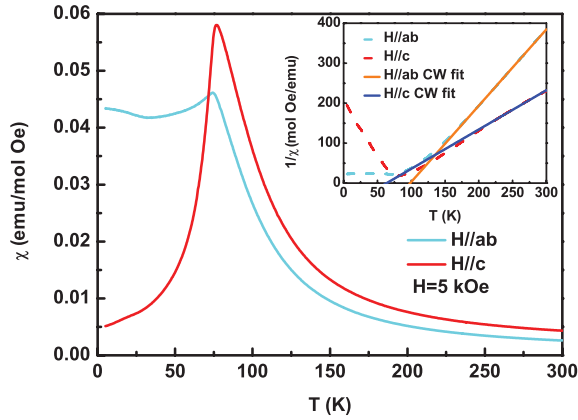


FIG. 1. (Color online) Temperature-dependent magnetic susceptibilities along the ab plane and the c axis in 5 kOe. The inset is the Curie-Weiss fits to the high-temperature parts of the susceptibilities.

to be $1.0\mu_B$ for $\mathbf{H} \parallel ab$ and $1.4\mu_B$ for $\mathbf{H} \parallel c$. A positive Weiss temperature generally indicates ferromagnetic coupling between the moments. We notice that many compounds with a crystal structure similar to CaCo_2As_2 show FM ordering in the basal planes, such as CaCo_2P_2 , LaCo_2P_2 , CeCo_2P_2 , PrCo_2P_2 , and NdCo_2P_2 .^{21,22} Especially, local-density approximation calculation (LDA) reveals that BaCo_2As_2 displays an in-plane ferromagnetic correlation even if it does not exhibit magnetic order above 1.8 K.¹⁹ So it is reasonable to infer that the moments of Co atoms are ordered ferromagnetically within the ab plane in its magnetic state. However, the magnetic structure of CaCo_2As_2 cannot be determined exactly by the static susceptibilities. The simplest supposition of the magnetic structure of CaCo_2As_2 is an A-type antiferromagnetism as shown in Fig. 6(a), which means the magnetic moments of Co atoms are aligned antiferromagnetically along the c axis with the stacking sequence $+ - + -$. Another possible type of stacking sequence along the c axis is $+ + - -$, as shown in Fig. 6(b). This type of stacking sequence has been observed in PrCo_2P_2 and NdCo_2P_2 .^{21,22} Neutron experiments are needed to determine the exact magnetic structure of CaCo_2As_2 .

Figure 2 shows the resistivity for $\mathbf{I} \parallel ab$ as a function of temperature. ρ_{ab} decreases with decreasing temperature,

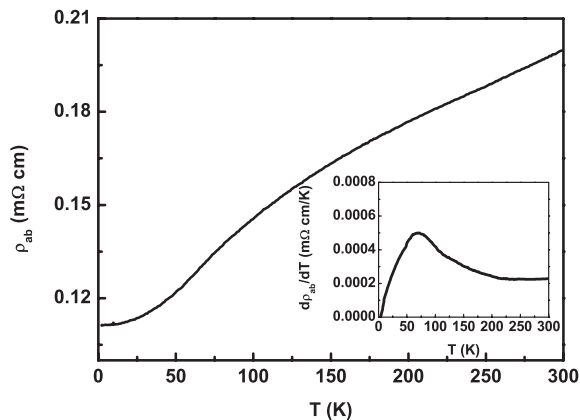


FIG. 2. Temperature-dependent resistivity of CaCo_2As_2 in zero field with $\mathbf{I} \parallel ab$. The inset is the derivative $d\rho_{ab}/dT$ as a function of temperature.

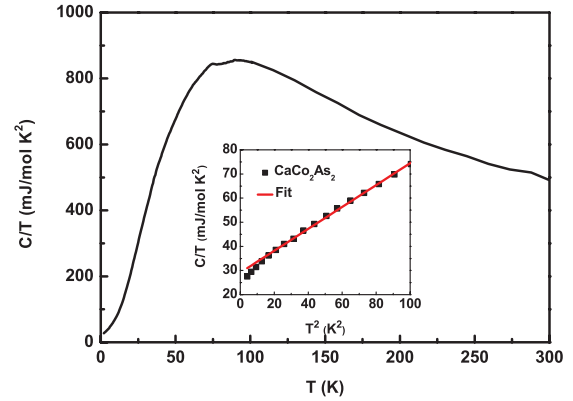


FIG. 3. (Color online) Temperature dependence of the specific heat of CaCo_2As_2 plotted as C/T vs T . The inset is a linear fit to the data below 10 K.

revealing a metallic behavior. There is no clear anomaly in the resistivity curve across the antiferromagnetic transition temperature. Only a broad peak could be seen in the derivative plot $d\rho_{ab}/dT$, as shown in the inset of Fig. 2. This is very different from the electronic transport behaviors of parent compounds of iron-based superconductors, where clear anomalies were observed in resistivity at the transition temperature.^{12,13} The absence of a similar anomaly in ρ_{ab} of CaCo_2As_2 indicates that the coupling between the conducting carriers and antiferromagnetic order in CaCo_2As_2 is much weaker than that of iron pnictide parents.

Temperature-dependent specific heat is shown in Fig. 3. Although the contribution of the phonon specific heat is dominant, we can clearly observe a weak peak located at around 76 K. It gives another evidence for a bulk long-range antiferromagnetic transition. The fit to low-temperature specific heat data is shown in the inset of Fig. 3. A good linear T^2 -dependent behavior indicates that the low-temperature specific heat is mainly contributed by electrons and phonons. The fit yields the electronic coefficient $\gamma = 30 \text{ mJ/K}^2/\text{mol CaCo}_2\text{As}_2$ or $15 \text{ mJ/K}^2/\text{mol Co atom}$. The value, which is much larger than that of iron pnictide parents,^{23,24} suggests a high density of states (DOS) at the Fermi level. LDA calculation for BaCo_2As_2 reveals that an electronic DOS at the Fermi level is already large enough to lead to a mean-field stoner instability toward in-plane ferromagnetism.¹⁹ The large electronic specific-heat coefficient of CaCo_2As_2 may give us a clue to understand the in-plane ferromagnetism in its antiferromagnetic state.

Magnetic susceptibilities measured in different fields are shown in Figs. 4(a) and 4(b). $\chi_{ab}(T)$ [$\chi(T)$ with $\mathbf{H} \parallel ab$] reveals a rather weak field dependence up to 60 kOe. However, $\chi_c(T)$ [$\chi(T)$ with $\mathbf{H} \parallel c$] [Fig. 4(b)] shows strong field-dependent behaviors. The peak of $\chi_c(T)$ shifts to low temperature with increasing magnetic field. This is a characteristic feature of an antiferromagnetic transition. Below 20 kOe, $\chi_c(T)$ reveals a well-defined antiferromagnetic transition. However, at $\mathbf{H} = 30 \text{ kOe}$, a shoulder begins to appear at 50 K. With increasing \mathbf{H} , the low-temperature parts of $\chi_c(T)$ are elevated and a plateau begins to form. At 50 kOe, $\chi_c(T)$ shows a large plateau below 40 K, which indicates that the antiferromagnetic ordering state is heavily disturbed by the applied field. With

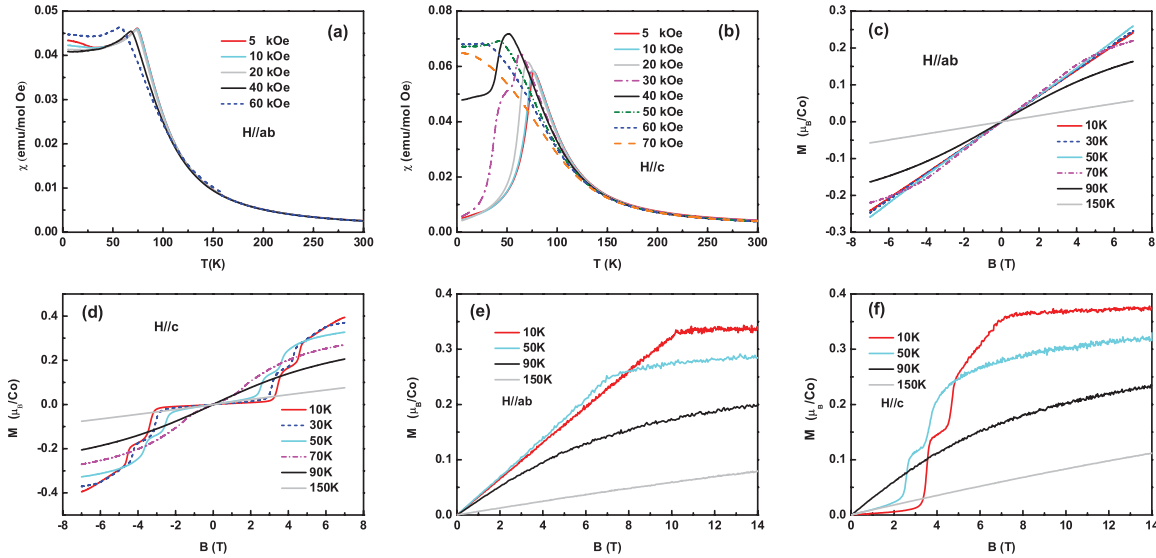


FIG. 4. (Color online) (a) and (b) Susceptibilities with $\mathbf{H} \parallel ab$ and $\mathbf{H} \parallel c$ in different fields. (c) and (d) Magnetization as a function of field from -7 to 7 T below and above T_N with $\mathbf{H} \parallel ab$ and $\mathbf{H} \parallel c$. (e) and (f) Magnetization as a function of field from 0 to 14 T below and above T_N with $\mathbf{H} \parallel ab$ and $\mathbf{H} \parallel c$.

further increasing magnetic field, the low-temperature plateau of $\chi_c(T)$ is gradually suppressed. At $\mathbf{H} = 70$ kOe, the plateau could not be seen clearly.

To understand these peculiar behaviors of $\chi_c(T)$, we collected the magnetization data measured as a function of field above and below T_N . Figure 4(c) shows $\mathbf{M}(\mathbf{H})$ with $\mathbf{H} \parallel ab$ in the range of -7 to 7 T. $\mathbf{M}_{ab}(10\text{ K})$ [$\mathbf{M}(\mathbf{H}, 10\text{ K})$ with $\mathbf{H} \parallel ab$] and $\mathbf{M}_{ab}(150\text{ K})$ exhibit a linear increase behavior as a function of applied magnetic field. $\mathbf{M}_{ab}(\mathbf{H})$ at 70 and 90 K deviate slightly from linear behavior. This anomaly originates from the strong magnetic fluctuation around the phase transition temperature. Figure 4(d) gives the results with $\mathbf{H} \parallel c$. Different from $\mathbf{H} \parallel ab$, $\mathbf{M}_c(10\text{ K})$ [$\mathbf{M}(\mathbf{H}, 10\text{ K})$ with $\mathbf{H} \parallel c$] undergoes two steep magnetization jumps at $\mu_0\mathbf{H}_{c1} = 3.5$ T and $\mu_0\mathbf{H}_{c2} = 4.7$ T. The first jump exhibits a notable hysteresis in the $\mathbf{M}-\mathbf{H}$ curve, as shown in Fig. 5. However, the second one at 4.7 T hardly shows a hysteresis. From 5 to 7 T, no hysteresis can be observed in $\mathbf{M}_c(10\text{ K})$. With increasing temperature, the two magnetization jumps become less pronounced and disappear above 70 K. $\mathbf{M}_c(\mathbf{H})$ at 150 K shows a good linear behavior as a function of magnetic field, indicating a typical paramagnetic response in paramagnetic states. We noticed that similar steep jump behaviors have been observed in many antiferromagnets, such as $\text{CuCl}_2 \cdot 2\text{H}_2\text{O}$,³ $\text{Cu}_2\text{MnSnS}_4$,⁵ $\text{BaCu}_2\text{Si}_2\text{O}_7$,⁷ $\beta\text{-Cu}_2\text{V}_2\text{O}_7$,⁸ and $\text{Na}_{0.85}\text{CoO}_2$.²⁵ A natural explanation for the steep magnetization jump behaviors in the antiferromagnet is a spin-flop transition. To yield more information on the jumps, we performed magnetization measurements up to 14 T.

Figures 4(e) and 4(f) show $\mathbf{M}_{ab}(\mathbf{H})$ and $\mathbf{M}_c(\mathbf{H})$ up to 14 T at different temperatures. At 10 K, $\mathbf{M}_{ab}(\mathbf{H})$ and $\mathbf{M}_c(\mathbf{H})$ display moment saturation behaviors at 10.2 and 7.6 T, respectively. The saturation moments are $0.33\mu_B$ per Co for $\mathbf{H} \parallel ab$ and $0.37\mu_B$ per Co for $\mathbf{H} \parallel c$. These values are much smaller than the effective moment per Co atom obtained from Curie-Weiss fits to the susceptibilities, indicative of an itinerant magnetism in CaCo_2As_2 . With increasing temperature, the

saturation behaviors are weakened and finally disappear above T_N .

It is well known that the spin-flop transition can be induced by a moderate magnetic field in an uniaxial antiferromagnet with low anisotropy. The first jump displays a notable hysteresis with increasing and then decreasing \mathbf{H} , indicating a first-order phase transition. We infer that this jump is ascribed to the traditional spin-flop transition which has been observed in many uniaxial antiferromagnets. The possible magnetic structures of CaCo_2As_2 in this spin-flop phase are shown in Figs. 6(c) and 6(d). At 4.7 T, another sudden jump occurs in $\mathbf{M}_c(\mathbf{H})$ at 10 K. This jump is unexpected from a simple uniaxial antiferromagnet. The steep increase of magnetization means that the magnetic structure of CaCo_2As_2 undergoes a sudden change. Different from the first jump, the second one exhibits much weaker hysteresis behavior. We cannot give a detailed description about this spin-flop transition because the exact magnetic structure and magnetic interaction in CaCo_2As_2 cannot be obtained from static susceptibility and

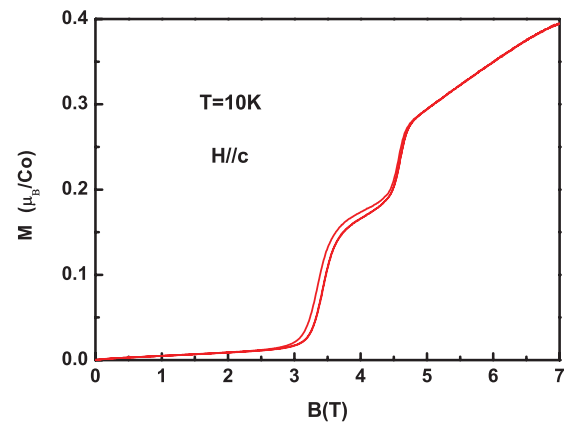


FIG. 5. (Color online) \mathbf{M}_c vs \mathbf{H} measured up to 7 T at 10 K with increasing and then decreasing \mathbf{H} .

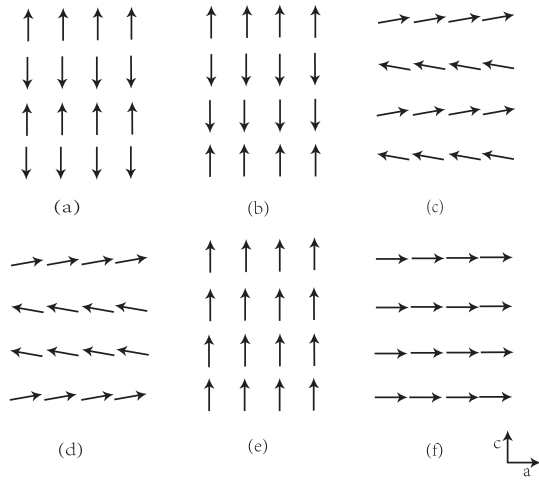


FIG. 6. (a) and (b) Two possible magnetic structures in CaCo_2As_2 . (c) and (d) Two possible spin-flop phases in CaCo_2As_2 . (e) Arrangement of Co moments in large field with $\mathbf{H} \parallel c$. (f) Arrangement of Co moments in large field with $\mathbf{H} \parallel ab$.

magnetization data. We think further neutron experiments are needed to settle this issue. For $\mathbf{H} \parallel ab$, the behaviors of the moments responding to the external field are much simpler than those of $\mathbf{H} \parallel c$. The balance between Zeeman energy, antiferromagnetic coupling energy, and magnetocrystalline anisotropic energy lead to the fact that the magnetic moments are gradually rotated to the ab plane. Above 10.2 T, all moments lie in the ab plane and are ordered ferromagnetically as shown in Fig. 6(f).

These interesting magnetic phenomena give us a chance to estimate the antiferromagnetic exchange energy along the c axis and the magnetocrystalline anisotropic energy in CaCo_2As_2 . The behavior of $\mathbf{M}_c(\mathbf{H})$ in magnetic states is mainly determined by interlayer antiferromagnetic exchange coupling energy $E_c = \sum_{ij} J_c \mathbf{S}_i \cdot \mathbf{S}_j$ and Zeeman energy $E_z = -\sum_i \mathbf{m}_i \cdot \mathbf{B}$ and magnetocrystalline anisotropic energy. J_c is the coupling constant. \mathbf{S} and \mathbf{m} are the spin and moments of Co ions, respectively. The saturation behavior above 7.6 T in $\mathbf{M}_c(10 \text{ K})$ manifests that the moments of Co atoms are all aligned ferromagnetically along the c axis, as shown in Fig. 6(e). At 7.6 T, we assume that the energy gain of the Zeeman interaction can just overcome the energy cost induced by the antiferromagnetic exchange coupling when the moments are flipped. In this method, we find a simply approximate relation: $E_z = -2E_c$ at $\mu_0 \mathbf{H} = 7.6 \text{ T}$ for $\mathbf{H} \parallel c$. Taking the estimated value of $m \sim 0.4\mu_B$ from the magnetization saturation and assuming $g = 2$, we estimate $J_c \sim 2 \text{ meV}$. Neutron-scattering data reveal that J_c in 122 parent

compounds of iron-based superconductors varies from 1 to 10 meV.²⁶ Our estimation about J_c in CaCo_2As_2 exhibits the same order of magnitude with 122 parent compounds.

J_c in CaCo_2As_2 is much lower than that of some other antiferromagnets, such as $\text{Na}_{0.85}\text{CoO}_2$, whose J_c as determined by neutron diffraction is 12.2 meV.²⁷ In $\text{Na}_{0.85}\text{CoO}_2$, a spin-flop transition was observed, which is very similar to the first spin-flop transition in CaCo_2As_2 .²⁵ But up to 14 T, the saturated phenomenon of $\mathbf{M}_c(5 \text{ K})$ in $\text{Na}_{0.85}\text{CoO}_2$ had not been observed. This means that J_c in $\text{Na}_{0.85}\text{CoO}_2$ is too high for 14 T to induce a similar magnetization saturation which occurs in CaCo_2As_2 .

The magnetization saturation behaviors for $\mathbf{H} \parallel ab$ and $\mathbf{H} \parallel c$ provide some information on the magnetocrystalline anisotropy. That the moments of Co atoms are aligned along the c axis at zero field indicates that it will cost more energy when the moments lie in the ab plane. To achieve the magnetic state as shown in Fig. 6(e), the Zeeman energy must overcome the energy cost caused by the magnetic exchange interaction when the moments are flipped. However, to achieve the magnetic state as shown in Fig. 6(f) with $\mathbf{H} \parallel ab$, the Zeeman energy must overcome the extra energy cost induced by magnetocrystalline anisotropic energy. This magnetocrystalline anisotropic energy can be estimated through the difference between the saturation fields of $\mathbf{H} \parallel ab$ and $\mathbf{H} \parallel c$. In this method, the magnetocrystalline anisotropic energy is estimated to be about $3.76 \times 10^5 \text{ erg/g}$.

IV. SUMMARY

In summary, we have investigated the transport and magnetic properties of single-crystalline CaCo_2As_2 by means of resistivity, heat capacity, magnetic susceptibility, and magnetization measurements. Our results reveal that CaCo_2As_2 undergoes an antiferromagnetic transition at $T_N = 76 \text{ K}$. The estimated value of the ordered moment on a Co atom is about $0.4\mu_B$. Two successive spin-flop transitions have been observed at $\mu_0 \mathbf{H}_{c1} = 3.5 \text{ T}$ and $\mu_0 \mathbf{H}_{c2} = 4.7 \text{ T}$ in $\mathbf{M}_c(10 \text{ K})$. Our analyses indicate that antiferromagnetic coupling between the ab plane is rather weak. The interlayer antiferromagnetic coupling constant and the magnetocrystalline anisotropic energy are estimated to be about 2 meV and $3.76 \times 10^5 \text{ erg/g}$, respectively.

ACKNOWLEDGMENTS

This work was supported by the National Science Foundation of China (10834013, 11074291) and the 973 project of the Ministry of Science and Technology of China (2011CB921701).

¹C. J. Gorter, *Rev. Mod. Phys.* **22**, 277 (1953).

²A. N. Bodganov, A. V. Zhuravlev, and U. K. Rößler, *Phys. Rev. B* **75**, 094425 (2007).

³C. J. Gorter, *Rev. Mod. Phys.* **25**, 332 (1953).

⁴U. Welp, A. Berger, D. J. Miller, V. K. Vlasko-Vlasov, K. E. Gray, and J. F. Mitchell, *Phys. Rev. Lett.* **83**, 4180 (1999).

⁵T. Fries, Y. Shapira, F. Palacio, M. C. Morón, G. J. McIntyre, R. Kershaw, A. Wold, and E. J. McNiff, Jr., *Phys. Rev. B* **56**, 5424 (1997).

⁶Y. Shapira and S. Foner, *Phys. Rev.* **170**, 503 (1968).

⁷I. Tsukada, J. Takeya, T. Masuda, and K. Uchinokura, *Phys. Rev. Lett.* **87**, 127203 (2001).

- ⁸Z. He and Y. Ueda, *Phys. Rev. B* **77**, 052402 (2008).
- ⁹D. A. Zocco, J. J. Hamlin, T. A. Sayles, M. B. Maple, J. H. Chu, and I. R. Fisher, *Phys. Rev. B* **79**, 134428 (2009).
- ¹⁰R. W. Wang, D. L. Mills, Eric E. Fullerton, J. E. Mattson, and S. D. Bader, *Phys. Rev. Lett.* **72**, 920 (1994).
- ¹¹Y. Kamihara, T. Watanabe, M. Hirano, and H. Hosono, *J. Am. Chem. Soc.* **130**, 3296 (2008).
- ¹²G. F. Chen, Z. Li, D. Wu, G. Li, W. Z. Hu, J. Dong, P. Zheng, J. L. Luo, and N. L. Wang, *Phys. Rev. Lett.* **100**, 247002 (2008).
- ¹³M. Rotter, M. Tegel, and D. Johrendt, *Phys. Rev. B* **78**, 020503(R) (2008).
- ¹⁴Z. A. Ren, W. Lu, J. Yang, W. Yi, X. L. Shen, Z. C. Li, G. C. Che, X. L. Dong, L. L. Sun, F. Zhou, and Z. X. Zhao, *Chin. Phys. Lett.* **25**, 2215 (2008).
- ¹⁵H. Ohta and K. Yoshimura, *Phys. Rev. B* **80**, 184409 (2009).
- ¹⁶V. P. S. Awana, I. Nowik, A. Pal, K. Yamaura, E. Takayama-Muromachi, and I. Felner, *Phys. Rev. B* **81**, 212501 (2010).
- ¹⁷M. A. McGuire, D. J. Gout, V. O. Garlea, A. S. Sefat, B. C. Sales, and D. Mandrus, *Phys. Rev. B* **81**, 104405 (2010).
- ¹⁸A. Marcinkova, D. A. M. Grist, I. Margiolaki, T. C. Hansen, S. Margadonna, and J.-W. G. Bos, *Phys. Rev. B* **81**, 064511 (2010).
- ¹⁹A. S. Sefat, D. J. Singh, R. Jin, M. A. McGuire, B. C. Sales, and D. Mandrus, *Phys. Rev. B* **79**, 024512 (2009).
- ²⁰X. F. Wang, T. Wu, G. Wu, H. Chen, Y. L. Xie, J. J. Ying, Y. J. Yan, R. H. Liu, and X. H. Chen, *Phys. Rev. Lett.* **102**, 117005 (2009).
- ²¹M. Reehuis, W. Jeitschko, G. Kotzyba, B. Zimmer, and X. Hu, *J. Alloys Compd.* **266**, 54 (1998).
- ²²M. Reehuis, P. J. Brown, W. Jeitschko, M. H. Möller, and T. Vomhof, *J. Phys. Chem. Solids* **54**, 469 (1993).
- ²³G. F. Chen, Z. Li, J. Dong, G. Li, W. Z. Hu, X. D. Zhang, X. H. Song, P. Zheng, N. L. Wang, and J. L. Luo, *Phys. Rev. B* **78**, 224512 (2008).
- ²⁴G. F. Chen, W. Z. Hu, J. L. Luo, and N. L. Wang, *Phys. Rev. Lett.* **102**, 227004 (2009).
- ²⁵J. L. Luo, N. L. Wang, G. T. Liu, D. Wu, X. N. Jing, F. Hu, and T. Xiang, *Phys. Rev. Lett.* **93**, 187203 (2004).
- ²⁶D. C. Johnston, *Adv. Phys.* **59**, 803 (2010).
- ²⁷L. M. Helme, A. T. Boothroyd, R. Coldea, D. Prabhakaran, A. Stunault, G. J. McIntyre, and N. Kernavanois, *Phys. Rev. B* **73**, 054405 (2006).